High-Pressure Elasticity of α-Quartz: Instability and Ferroelastic Transition

Eugene Gregoryanz,[1] Russell J. Hemley,[1] Ho-kwang Mao,[1] and Philippe Gillet[2]

[1]*Geophysical Laboratory and Center for High Pressure Research, Carnegie Institution of Washington, 5251 Broad Branch Road NW, Washington, D.C. 20015*

[2]*Laboratoire de Sciences de la Terre, École Normale Supérieure de Lyon, 69364 Lyon cedex O7, France*

(Received 4 October 1999)

The single-crystal elastic moduli of α-quartz were measured to above 20 GPa in a diamond-anvil cell by Brillouin spectroscopy. The behavior of the elastic moduli indicates that the high-pressure phase transition in quartz is ferroelastic in nature and is driven by softening of C_{44} through one of the Born stability criteria. The trends in elastic moduli confirm theoretical predictions, but there are important differences, particularly with respect to the magnitudes of the B_i. The quartz I-II transition occurs prior to complete softening of the mode and amorphization.

PACS numbers: 62.50.+p, 61.50.Ks, 62.20.Dc, 78.35.+c

The discovery of pressure-induced amorphization of ice [1] and the subsequent observation of related transitions in other materials have provided numerous insights into the metastable behavior of materials under pressure. Like ice, SiO_2 forms tetrahedral framework structures at low pressures [2], which also serve as a model system for the studies of phase transitions, vibrational dynamics, and chemical bonding in general. α-quartz, the most common and extensively studied phase of silica, was found to undergo pressure-induced amorphization [3,4] shortly after the discovery in ice. Since then, the transition in α-quartz has been extensively investigated experimentally (e.g., Refs. [5–7]). The notion that pressure-induced amorphization in α-quartz (and materials in general [8]) is driven by an intrinsic instability in the structure was suggested by the negative pressure derivatives of one of the elastic moduli [3,4]. Subsequent work has revealed additional complexity that is not fully understood. This includes the appearance of abrupt changes in microstructure (macroscopic and microscopic planar features) beginning at 18 GPa [6] and a crystalline-crystalline transformation (quartz I-II) that precedes complete amorphization [7]. The relationship between a possible instability in the structure leading to amorphization and both the onset of the microstructural changes and the I-II transition has not been established.

The problem has been examined theoretically (e.g., Refs. [9–16]). One of the first theoretical studies of quartz amorphization identified an instability that was attributed to the shortening of the nearest O-O distances [12]. Molecular dynamics simulations of Tse *et al.* [11] predicted an instability at 22.3 GPa, indicating that one of the Born stability criteria (B_2) [17] is violated at that pressure, which corresponded to the point where the elastic modulus C_{33} suddenly decreases. Subsequent classical interatomic and first-principles calculations by Binggeli *et al.* [10] suggested that the elastic instability is associated with Born criteria B_3 which decreases with pressure and becomes negative at about 30 GPa. They concluded that the reported B_2 instability [11] is not the cause but rather the result of the transition. They also predicted that none of the individual elastic moduli vanish in the pressure region of quartz amorphization and concluded that vanishing of C_{66} or C_{44} is not the cause of the instability. A dynamical (zone edge) instability is predicted to be close in pressure to the elastic (zone center) instability along the same acoustic branch [18,19]. The I-II transition has also been the subject of numerous theoretical studies (e.g., [16]). The transformation exhibits order-disorder character with some parallels to the α-β transition but is still not fully understood.

Measurements of the elasticity of quartz at high pressure are required to address these questions. Ultrasonic techniques have been used to determine the single-crystal elasticity tensor of α-quartz at and near ambient pressure [20,21], but they have not been developed and applied at the pressures required for examining these phenomena in quartz. Brillouin spectroscopy probes elastic waves propagating in a crystal and can be used to determine the individual elastic moduli. The technique is readily adapted to diamond-anvil cells (e.g., Refs. [22,23]) for studies of materials in the pressure range of quartz amorphization. Notably, the determination of the pressure dependence of the elastic tensor requires the use of single-crystal techniques [23]. A Brillouin scattering study of SiO_2 was carried out above the quartz transformation pressure [5] and revealed information on the character of the pressure-amorphized sample. But because of the 180° geometry used in the experiment, the transverse modes were not observable, precluding determination of the individual C_{ij}. Here we report the first single-crystal Brillouin measurements of α-quartz to above 20 GPa at 300 K which yielded the values of the individual elastic constants as a function of pressure. The behavior of the C_{ij} with pressure shows that amorphization in α-quartz is driven by an elastic instability. We further show that the transition to the amorphous state is ferroelastic in nature.

We used a six-pass Brillouin spectrometer described elsewhere [23]. The $\lambda_0 = 514.5$ nm Ar^+-laser line was used as the excitation source. A polished ~ 30 μm thick,

~100 μm diameter sample of α-quartz and a ruby chip were loaded into a 200 μm stainless steel gasket hole of a large-aperture symmetric diamond-anvil cell. Neon was used as the pressure-transmitting medium in the first run from ambient to 15.5 GPa, and helium in the second run to 22 GPa. No noticeable difference between two runs was observed. The diamond cell was mounted on a stage which allowed rotation of the cell around χ angle (axis perpendicular to the plane of diamond culets). The large-aperture opening allowed Brillouin shift measurements over a large range of reciprocal space by rotation of the cell around χ. The data were collected in the forward 60° scattering geometry where incident and scattered angles are equal [22]. The symmetry of this geometry simplifies the Brillouin equation and allows calculation of the elastic constants without knowledge of refractive index [22]. At each pressure up to 18 spectra were collected in 10° intervals as a function of χ. At every angle, the longitudinal and one transverse mode were observable and at 4–5 angles both transverse modes were seen. The crystallographic orientation of the sample was determined *in situ* by x-ray diffraction.

The longitudinal and transverse shifts as a function of χ angle are shown in Fig. 1. With increasing pressure the frequency shift of the longitudinal and fast transverse mode increases. In contrast, the frequency of the slow transverse mode decreases with pressure. The measured frequencies of the Brillouin shifts obtained on decompression from 15 GPa are largely indistinguishable from those obtained on compression (see also Ref. [5]). The intensities of transverse modes varied with crystallographic direction and at some angles were comparable with those of the longitudinal modes at every pressure up to ~17 GPa.

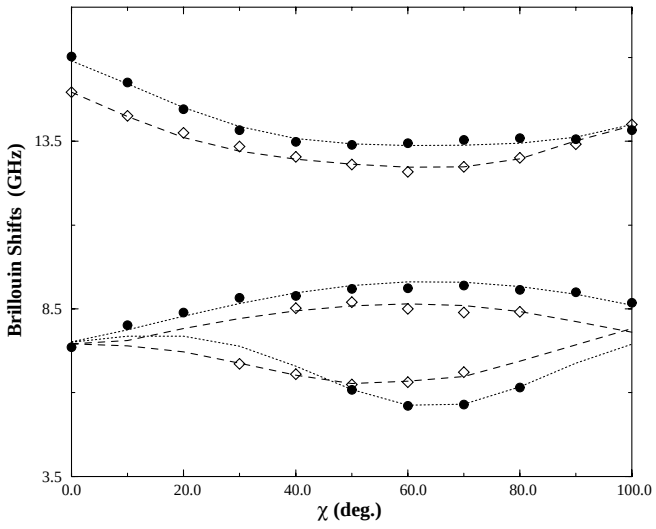

FIG. 1. Longitudinal and transverse frequency shifts as a function of χ (about an arbitrary reference) at 5.0 (open) and 20.2 (filled) GPa. The errors in frequency measurements are comparable with the symbol size. The curves are calculated from the best fit elastic moduli.

With further increase in pressure, the intensities of transverse modes decreased slowly while the background rose. In this range of pressure, the previously noted planar features were observed [6,7]. When the pressure was raised to ~20.8 GPa, lamellae [6] developed in the sample. At this pressure, some parts of the sample were still crystalline and it was possible to collect spectra. When the pressure was increased to 21.5 GPa, the spectra deteriorated, precluding the accurate measurement of Brillouin shifts.

The single-crystal elastic moduli (C_{ij}) were determined using a least-squares fitting routine which minimizes the difference between measured and calculated frequency shifts by parameter searches through the elastic moduli space [24]. The density of quartz needed for the elastic moduli calculations was obtained from x-ray measurements of the equation of state over this pressure range [25]. The initial guess for the elastic constants at each pressure was the set of C_{ij} values at lower pressure. In general, the calculation of the effective elastic constants in piezoelectric media requires consideration of the electrical conditions because of the electric field associated with the sound wave. However, the effect of piezoelectricity in quartz can be neglected because of its small coupling ($k \sim 0.01$ or less) with sound waves [26]. The stress-strain relation modified by piezoelectricity is written as

$$T_{ij} = C_{ijkl} S_{kl} - e_{nij} E_n . \quad (1)$$

Here T_{ij} is the stress tensor, S_{kl} the strain tensor, E_n electric field, C_{ijkl} the elastic constants tensor, and e_{nij} the piezoelectric tensor. The analysis of Eq. (1) shows (see Ref. [27]) that the effect of piezoelectricity in α-quartz leads to overestimation by ~0.6% in C_{11} and underestimation by ~5% in $C_{12} = C_{11} - 2C_{66}$. These are the constants expected to be affected the most by the effect of piezoelectricity due to the relatively large value of e_{11} [27]. C_{44} is weakly coupled through e_{14} because e_{14} is much smaller than e_{11}. On the other hand, C_{33} is free from piezoelectric coupling since $e_{3j} = 0$.

The single-crystal elastic moduli of α-quartz as a function of pressure are shown in Fig. 2. The C_{ij} at zero pressure are in a good agreement with the values obtained from ultrasonic measurements [20]. All moduli increase with pressure except C_{44}, which steadily decreases but remains positive over the investigated pressure range. McSkimin *et al.* [20] found that C_{66} decreased with pressure up to 0.2 GPa; a linear extrapolation of the C_{ij} to zero gives an instability at 15 GPa (see Ref. [4]). In contrast, we find a positive pressure shift for the C_{66} at all of our measured pressures. Extrapolating the data to higher pressure (beyond the I-II transition) indicates that C_{44} would vanish at 39 GPa. Interestingly, C_{14} changes sign near 12 GPa and pressure dependence of C_{33} appears to become nonlinear at higher pressures [28].

The mechanical stability of a crystal requires examination of the Born stability criteria [17] which provide

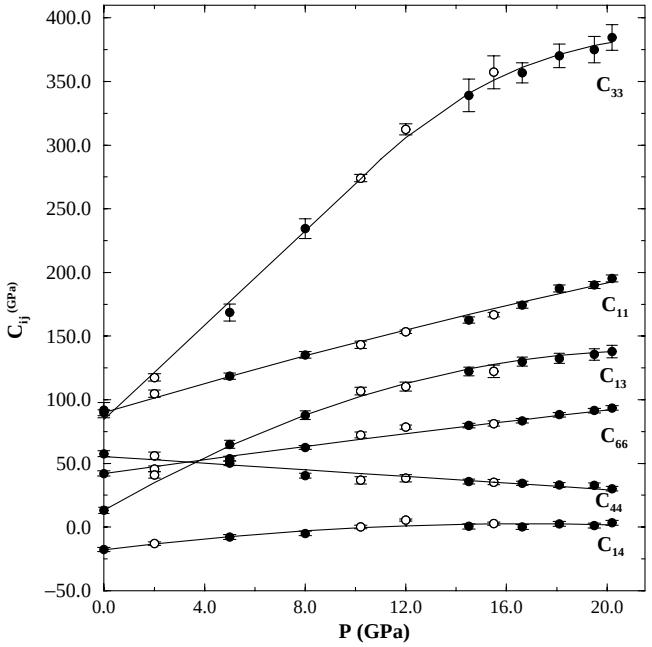

FIG. 2. Individual C_{ij} of α-quartz as a function of pressure. The solid circles represent increasing pressure and open circles decreasing pressure. The solid curves show fits to the data. The errors in elastic moduli without error bars are comparable to (or less than) the symbol size. The error bars represent the standard deviation in the best fit parameters and uncertainties in the frequency shifts and crystal orientation.

the necessary conditions for a crystal to be mechanically stable. These criteria translate into the condition that the elastic constant matrix is positive, which for a trigonal crystal is

$$\begin{aligned} B_1 &= C_{11} - |C_{12}| > 0, \\ B_2 &= (C_{11} + C_{12})C_{33} - 2C_{13}^2 > 0, \\ B_3 &= (C_{11} - C_{12})C_{44} - 2C_{14}^2 > 0. \end{aligned} \tag{2}$$

Figure 3 shows the experimental pressure dependence of the Born criteria for α-quartz. B_1 and B_2 both increase within the investigated pressure range while B_3 goes through a maximum around 17 GPa and then decreases. However, the elastic constants and Born stability remain finite at pressures corresponding to the appearance of planar features (18 GPa) and the I-II transition (22 GPa) which prevented higher pressure single-crystal measurements. Extrapolation in pressure indicates that B_3 becomes negative at about 39 GPa. Qualitatively, the experimentally determined pressure dependences of the three Born stability criteria show similar behavior to those calculated theoretically [10], but there are important quantitative differences. In particular, the calculations with pseudopotentials give $B_3 = 0$ at 35 GPa and with interatomic pair potentials at 22 GPa. Notably, the instability at 22 GPa calculated with interatomic potentials and the observation of the I-II transition at that pressure is coincidental because the experimental B_3 is finite at that pressure.

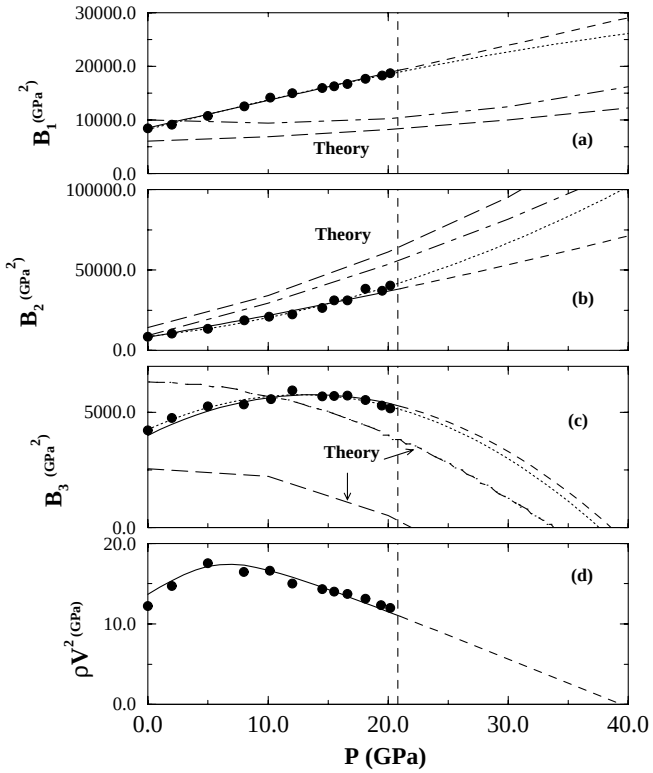

FIG. 3. Born criteria (a)–(c) and soft acoustic mode (d) of α-quartz as a function of pressure. The solid circles were calculated from the measured elastic moduli. The solid lines were calculated from individual fits to the C_{ij}. The dot-dashed and dashed lines show the result of pseudopotentials and interatomic potentials calculations, respectively, from Ref. [10]. The dashed lines are extrapolations of the present data using linear pressure fits to the C_{ij}. The dotted lines are quadratic fits to the B_i. Nearly identical behavior is found for the calculated instability when using quadratic fits to the C_{ij} ($B_3 = 0$ at ~45 GPa). The vertical dotted line shows the position of the quartz I-II transition at 20.8 GPa.

It is possible to identify the type of the phase transition by investigating the combination of the elastic constants corresponding to the soft mode frequency which vanishes at the transition. If we examine the behavior of the soft acoustic mode shown in Fig. 3 which for trigonal classes 32, $\bar{3}m$, and $3m$ is (see Ref. [29])

$$\begin{aligned} \rho V^2 = \tfrac{1}{4}\{&(C_{11} - C_{12} + 2C_{44}) \\ &- [(C_{11} - C_{12} - 2C_{44})^2 + 16C_{14}^2]^{1/2}\}. \end{aligned} \tag{3}$$

We see that ρV^2 goes through a maximum near 6.5 GPa and then decreases nearly linearly, vanishing at ~39 GPa. The linear behavior and negative slope of the mode in the higher pressure regime is indicative of proper ferroelastic behavior.

In conclusion, measurement of the single-crystal elastic moduli of α-quartz has provided the first complete *in situ* high-pressure study of C_{ij} and Born stability criteria of a material undergoing pressure-induced amorphization. It has revealed an elastic instability in α-quartz associated with the softening of C_{44} with pressure. The soft mode

analyses indicates an underlying ferroelastic transition. The I-II transition, which intercedes prior to complete softening of the mode, may be triggered by an associated dynamical instability (e.g., Refs. [18,19]). The role of other factors such as thermal activation, preexisting planar defects, and the precise crystal structure of phase II also needs to be clarified. To this end, our measurements provide stringent tests of first-principles theoretical models of the high-pressure behavior of this material.

We thank M. A. Carpenter for very useful discussions, and J. Badro, L. Finger, M. Eremets, and S. Gramsch for experimental assistance and comments on the manuscript. This work was supported by the N.S.F.

[1] O. Mishima, L. D. Calvert, and E. Whalley, Nature (London) **310**, 393 (1984).
[2] *Silica-Physical Behavior, Geochemistry and Material Applications,* edited by P. J. Heaney, C. T. Prewitt, and G. V. Gibbs, Reviews in Mineralogy, Vol. 29 (Mineralogical Society of America, Washington, DC, 1994).
[3] R. J. Hemley, *High-Pressure Research in Mineral Physics,* edited by M. H. Manghnani and Y. Syono (Terrapub, Tokyo-A.G.U., Washington, DC, 1987), p. 347.
[4] R. J. Hemley, A. P. Jephcoat, H. K. Mao, L. C. Ming, and M. H. Manghnani, Nature (London) **334**, 52 (1988).
[5] L. McNeil and M. Grimsditch, Phys. Rev. Lett. **68**, 83 (1992).
[6] K. J. Kingma, C. Meade, R. J. Hemley, H. K. Mao, and D. R. Veblen, Science **259**, 666 (1993); P. Cordier, J. Doukhan, and J. Peryonneau, Phys. Chem. Miner. **20**, 176 (1993).
[7] K. J. Kingma, R. J. Hemley, H. K. Mao, and D. R. Veblen, Phys. Rev. Lett. **70**, 3927 (1993).
[8] P. Richet and P. Gillet, Eur. J. Mineral. **9**, 907 (1997).
[9] S. Tsuneyuki, Y. Matsui, H. Aoki, and M. Tsukada, Nature (London) **339**, 209 (1989).
[10] N. Binggeli and J. R. Chelikowsky, Phys. Rev. Lett. **69**, 2220 (1992).
[11] J. S. Tse and D. D. Klug, Phys. Rev. Lett. **67**, 3559 (1991).
[12] J. R. Chelikowsky *et al.,* Phys. Rev. Lett. **65**, 3309 (1990).
[13] S. L. Chaplot and S. K. Sikka, Phys. Rev. B **47**, 5710 (1993).
[14] J. Badro, P. Gillet, and J. L. Barrat, Europhys. Lett. **42**, 643 (1998).
[15] N. Ovsyuk and S. Goryainov, Phys. Rev. B **60**, 14 481 (1999).
[16] M. S. Somayazulu, S. M. Sharma and S. K. Sikka, Phys. Rev. Lett. **73**, 98 (1994); J. Tse, D. D. Klug, Y. Le Page, and M. Bernasconi, Phys. Rev. B **56**, 10 878 (1997); I. Svishchev, P. Kusalik, and V. Murashov, Phys. Rev. B **55**, 721 (1997); R. M. Wentzcovitch, C. da Silva, J. R. Chelikowsky, and N. Binggeli, Phys. Rev. Lett. **80**, 2149 (1998).
[17] M. Born and K. Huang, *Dynamical Theory of Crystal Lattices* (Oxford University Press, London, 1954).
[18] S. L. Chaplot and S. K. Sikka, Phys. Rev. Lett. **71**, 2674 (1993); N. Binggeli and J. R. Chelikowsky, *ibid.* **71**, 2675 (1993).
[19] G. W. Watson and S. C. Parker, Philos. Mag. Lett. **71**, 59 (1985).
[20] H. J. McSkimin, P. Andreatch, and R. N. Thurston, J. Appl. Phys. **36**, 1624 (1965).
[21] A. G. Smagin and B. G. Mil'shtein, Sov. Phys. Crystallogr. **19**, 514 (1975).
[22] C. Whitfield, E. Brody, and W. A. Bassett, Rev. Sci. Instrum. **47**, 942 (1976).
[23] C. S. Zha, T. S. Duffy, H. K. Mao, and R. J. Hemley, Phys. Rev. B **48**, 9246 (1993).
[24] The procedure is described in detail in E. Gregoryanz, M. J. Clouter, N. Rich, and R. Goulding, Phys. Rev. B **58**, 2497 (1998).
[25] K. J. Kingma, Ph.D. thesis, Johns Hopkins University, 1994.
[26] T. Ikeda, *Fundamentals of Piezoelectricity* (Oxford University Press, Oxford, 1996).
[27] I. Ohno, Phys. Chem. Miner. **17**, 371 (1990).
[28] Further details are described in E. Gregoryanz *et al.* (to be published).
[29] M. A. Carpenter and E. K. H. Salje, Eur. J. Mineral. **10**, 693 (1998).